

Novel Smad proteins localize to IR-induced double-strand breaks: interplay between TGF β and ATM pathways

Minli Wang¹, Janapriya Saha¹, Megumi Hada¹, Jennifer A. Anderson², Janice M. Pluth³, Peter O'Neill² and Francis A. Cucinotta^{4,*}

¹USRA Division of Life Sciences, Houston, TX 77058, USA, ²Gray Institute for Radiation Oncology and Biology, Oxford University, Oxford OX37DQ, UK, ³Lawrence Berkeley National Laboratory, Berkeley, CA 94720, USA and ⁴NASA Space Radiation Program, Lyndon B. Johnson Space Center, Houston, TX 77058, USA

Received August 10, 2012; Revised October 1, 2012; Accepted October 6, 2012

ABSTRACT

Cellular damage from ionizing radiation (IR) is in part due to DNA damage and reactive oxygen species, which activate DNA damage response (DDR) and cytokine signaling pathways, including the ataxia telangiectasia mutated (ATM) and transforming growth factor (TGF) β /Smad pathways. Using classic double-strand breaks (DSBs) markers, we studied the roles of Smad proteins in DDR and the crosstalk between TGF β and ATM pathways. We observed co-localization of phospho-Smad2 (pSmad2) and Smad7 with DSB repair proteins following low and high linear energy transfer (LET) radiation in human fibroblasts and epithelial cells. The decays of both foci were similar to that of γ H2AX foci. Irradiation with high LET particles induced pSmad2 and Smad7 foci tracks indicating the particle trajectory through cells. pSmad2 foci were absent in S phase cells, while Smad7 foci were present in all phases of cell cycle. pSmad2 (but not Smad7) foci were completely abolished when ATM was depleted or inactivated. In contrast, a TGF β receptor 1 (TGF β R1) inhibitor abrogated Smad7, but not pSmad2 foci at DSBs sites. In summary, we suggest that Smad2 and Smad7 contribute to IR-induced DSB signaling in an ATM or TGF β R1-dependent manner, respectively.

INTRODUCTION

Ionizing radiation (IR) produces DNA damage and reactive oxygen species (ROS), which activate DNA damage response (DDR) and cytokine signaling pathways, and may lead to cell death, mutation or genomic instability (1–5). High linear energy transfer

(LET), high charge and energy particle radiation produce a characteristic track structure consisting of high energy deposition in biomolecules near the particle trajectory and a diffused radiation of low LET secondary electrons called δ -rays (2,3). For high LET radiation, there is evidence of increased contributions from clustered double-strand breaks (DSBs), and complex DNA damages with distinct protein signaling kinetics compared with low LET radiation (4). In addition, the types and spatial distributions of ROS vary with LET (5). Thus, high LET radiation may serve as a tool to investigate the possible crosstalk between the DDR and other signaling pathways.

Two well-known DSB repair pathways in vertebrate cells are non-homologous end joining (NHEJ) and homologous recombination (HR). NHEJ mainly occurs throughout the cell cycle but is the primary pathway in G1 and early S phase. The major proteins in the canonical NHEJ pathway are DNA-PK, DNA ligase IV/XRCC4/XLF4 complex, with poly (ADP-ribose) polymerase (PARP) and DNA ligase III/XRCC1 proteins playing a role in a backup NHEJ pathway (6–9). HR is believed to be active in late S and G2 phase, with RAD51 and its paralogs playing major roles in this pathway (10). Ataxia telangiectasia mutated (ATM) is a crucial mediator for DSB responses, activated by autophosphorylation upon DSB induction and critical for phosphorylating a number of proteins involved in DSB repair and damage signaling pathways (11). DSB sensing and processing proteins induced by IR can be observed by immunofluorescence and are referred to as IR-induced foci (IRIF) (12). IRIF may contain many proteins involved in ongoing repair or checkpoint control, such as γ H2AX, 53BP1, RAD51, Chk2 and ATF2 (13–15). Studies have revealed monitoring γ H2AX as a fairly accurate means to estimate the formation and loss of DSBs formation at different times (8,16,17).

*To whom correspondence should be addressed. Tel: +1 281 483 0968; Fax: +1 281 483 3058; Email: francis.a.cucinotta@nasa.gov

Besides inducing DSBs, IR also generates ROS that can activate cytokine signaling pathways involving transforming growth factor (TGF) β (18). The well-described TGF β /Smads signaling pathway has been shown to be important in cellular and tissue processes, including cell growth, proliferation, differentiation and apoptosis (19). In non-stimulated cells, the receptor-associated Smads designated R-Smad1, 2, 3, 5 and 8 are located predominantly in the cytoplasm (20). Once activated, the TGF β receptor complex aids in phosphorylation of the R-Smads, which then complex with co-Smad4 and allow the translocation of R-Smads to the nucleus to activate targeted gene expression (21). Upon completion of this task, Smad2 is targeted for degradation or de-phosphorylation and exported out of the nucleus (22,23). Inhibitory Smad (Smad7) is not phosphorylated following TGF β activation as it lacks the type I receptor phosphorylation site (24). It is a general antagonist of TGF β signaling and regulates the formation of Smad2/Smad4 complexes, blocking the nuclear accumulation of Smad2 and 3. It also binds to Smurf2 to form an E3 ubiquitin ligase that targets the TGF β type I receptor for degradation, thereby inhibiting the activation of Smad2 (25). In addition, Smad7 was shown to interact with DNA through the MH2 domain and co-localize with γ H2AX at DNA damage sites in TGF β -treated mouse embryo fibroblasts (26).

A link between TGF β signaling and ATM phosphorylation was shown following irradiation previously (18). Inhibiting TGF β signaling in human cells prior to high doses of irradiation resulted in a reduction in ATM phosphorylation as well as reduced phosphorylation of TGF β substrates including p53, Chk2 and Rad17 (18). As a consequence of TGF β inhibition and resulting lack of ATM activation, few γ H2AX foci were detected after irradiation. These results suggested that either TGF β 'primes cells to respond to DNA damage' or that it aids in ATM activation (18). Studies have shown that while TGF β 1 is involved in ATM and p53 phosphorylation, both TGF β receptor 1 (TGF β R1) and Smad2 are not (27). A role for Smad7 in ATM activation was also noted by a Smad7-dependent increase in ATM S1981 phosphorylation in prostate cancer cells stimulated with TGF β 1 (26). γ H2AX and Smad7 co-localization following TGF β treatment suggest Smad7 may act as a scaffold for ATM and its substrate γ H2AX (26).

Although previous work has investigated how TGF β 1 modulates ATM activity, the precise mechanism, especially in the context of radiation, is not yet known. Using classic DSB markers of signaling and repair pathways (γ H2AX, 53BP1, pATF2 and RAD51), we have studied the roles of the Smad proteins in response to DNA damage and investigated their dependence on crosstalk between the TGF β and ATM pathways. We studied different qualities of radiation to investigate the possibility of distinct signaling components following simple or clustered DNA damage (11) or spatial distributions of ROS. The transition from low to high LET radiation was studied by varying the LET using different particle and energy exposures. The effect on different cell types (human esophageal epithelial and fibroblast cells)

was also investigated in the current work. Immunostaining was performed for various proteins forming IRIF, as well as western immunoblotting for Smad proteins to identify relationships between pathways. ATM kinase and TGF β signaling inhibitors were additionally used to study the interplay between radiation-induced DNA damage signaling and the TGF β /Smad pathway.

MATERIALS AND METHODS

Cell lines and chemicals

Human telomerase reverse transcriptase (TERT)-immortalized adult skin fibroblast cells (82-6 cells, courtesy of Judith Campisi, (28)) were grown in Dulbecco's modified Eagle's medium supplemented with 10% fetal bovine serum (FBS) and antibiotic-antimycotic. Human primary fibroblast cells (IMR90), a kind gift from Chuanyuan Li (Duke University, NC, USA), were maintained in modified eagle medium (MEM) supplemented with 10% FBS, 100 U/ml penicillin and 100 μ g/ml streptomycin and used at passage 8. hTERT-immortalized human esophageal epithelial cells (EPCs) were cultured as described previously (29). AT mutant cells (GM02052) were maintained in MEM supplemented with 15% FBS, L-glutamine and Pen-Strep.

Two nanograms per milliliter recombinant human TGF β 1 (PeproTech, Rocky Hill, NJ, USA), 10 μ M ATM kinase inhibitor KU55933 and 1 μ M TGF β R1 kinase inhibitor SD208 (Tocris Bioscience, Ellisville, MO, USA) were added to medium 1 h prior to radiation.

Irradiation

Experiments using particle irradiation were performed at the NASA Space Radiation Laboratory (NSRL) in Brookhaven National Laboratory (BNL, NY, USA). Oxygen (O) particles with an energy of 77 MeV/u, a LET of 58 keV/ μ m, iron (Fe) particles with an energy of 600 MeV/u and a LET of 180 keV/ μ m were delivered. A 20 \times 20 cm beam with a dose uniformity of \pm 2%, and a dose rate of \sim 0.5 Gy/min was used. 137 Cs gamma radiation (γ -rays) experiments were completed at NASA Lyndon B. Johnson Space Center (Houston, TX, USA) with a dose rate of 0.3 Gy/min. T25 flasks containing exponentially growing cells were exposed vertically with the cell surface perpendicular to the beam. Eight-well chamber slides were exposed either vertically or horizontally as indicated. All samples were irradiated at room temperature before returned to a 37°C incubator.

Western blotting and immunofluorescence

To detect nuclear-specific proteins, nuclear extracts were prepared using NE-PER Nuclear Protein Extraction Kit from Thermo Scientific (Rockford, IL, USA), supplemented with Halt protease inhibitor cocktail (Thermo Scientific). After electrophoresis in 10% sodium dodecyl sulfate-polyacrylamide gel electrophoresis and electroblotting (Bio-Rad, Hercules, CA, USA), the nitrocellulose membrane was processed according to the instructions of the manufacturer. Blots were incubated with primary antibodies and followed by goat anti-mouse/rabbit

immunoglobulin G conjugated to horseradish peroxidase (Amersham Bioscience). The membranes were probed using the ECL-Plus western blotting detection reagents as recommended by the manufacturer (GE Healthcare). The signal was detected using a Storm 840 scanner (GE Healthcare).

For immunofluorescence, cells were grown on LabTek eight-well chamber slides (Thermo Scientific) and fixed with 4% paraformaldehyde for 15 min. After permeabilization with 0.3% Triton X-100 in phosphate buffered saline (PBS) for 3 min, cells were blocked with 10% normal goat serum in PBS and incubated with the indicated primary antibodies, at 4°C overnight. Detection was accomplished using Alexa Fluor 488 or 594 conjugated secondary antibodies (Invitrogen) and nuclei were counterstained with 4',6-diamidino-2-phenylindole (DAPI). Immunofluorescence was evaluated with a fluorescence microscope Axioplan2 (Zeiss, Sweden).

Rabbit anti-phospho-Smad2 (pSmad2) (S465/S467) and rabbit anti-phospho-p53 were from Cell Signaling Technology Inc.; mouse anti-Smad1/2/3 antibody was from Santa Cruz Biotechnology; rabbit anti-phospho-Smad3 (S423+S425) was from Abcam; mouse anti-Smad7 was from R&D Systems; mouse anti-TATA-binding protein 1 (TBP1) and mouse anti- γ H2AX (S139) antibodies were from Millipore; rabbit anti-phospho-ATF2 (S490/498) antibody was from PhosphoSolutions; mouse anti-cyclin A and mouse anti-53BP1 antibodies were from BD Transduction Laboratories and rabbit anti-RAD51 antibody was from Calbiochem.

RESULTS

Similar radiation quality-dependent kinetics observed for pATF2 and γ H2AX

Fundamental studies have revealed that track structure signatures from high LET particle exposures can be identified by DSB repair phospho-proteins' kinetics, for proteins such as γ H2AX and pATF2 (15,30). Figure 1A illustrates the effect of radiation quality on the foci distribution at an early time after radiation in human fibroblast cells irradiated horizontally, which allows for identification of the particle trajectory through the cell. Low LET radiation such as γ -rays deposits their energy sparsely; therefore, γ H2AX foci are uniformly distributed instead of foci tracks. For particle exposure, irradiating vertically allows for an easier quantification of foci kinetics without attempting to define individual foci within a track as would be needed with a horizontal irradiation exposure (31). Nevertheless, each focus generated represents a number of DSBs which are in close proximity to each other. A LET-dependent decay in foci was observed after radiation, with slower DSB repair kinetics observed following high LET irradiation when compared with γ -ray exposed samples. Six hours after γ -rays nearly 25% of γ H2AX and pATF2 foci remain following low LET exposure whereas following high LET radiation ~40–50% of the foci remain at the same time point (Figure 1B).

Smad7 is recruited to DSB sites after both high and low LET radiation

We were interested in studying the crosstalk between TGF β /Smad signaling pathway and the DDR following radiation exposure. Thus, we investigated how different Smad proteins respond to radiation-induced DNA damage, in particular its difference in DNA damage quality following high LET radiation compared with γ -rays. As a key member of TGF β /Smad signaling, we first studied the inhibitory Smad7. Similar to γ H2AX and pATF2 foci, following high LET radiation, Smad7 foci localized to DSBs and showed similar kinetics when compared with these DSB repair proteins. Smad7 accumulated at the radiation tracks in human fibroblasts (82-6) detected 1 h after Fe particles and were visible up to 24 h after exposure (Figure 2A). Smad7 foci were present at DSBs sites in 82-6 cells after exposure to both high and low LET radiation of oxygen and γ -rays, respectively (Figure 2B and C). Similar to the kinetics in foci resolution observed with pATF2 and γ H2AX, high LET radiation caused a larger persistence of Smad7 foci when compared with low LET radiation (Figure 2D). The localization of Smad7 foci to the sites of DSBs is indicated by co-localization with known phospho-protein markers of DSBs-pATF2 (Figure 2B and C). The level of co-localization of Smad7 with pATF2 and RAD51 was quantified and analyzed in Figure 2G. Eighty-five percent of Smad7 were found co-localized with pATF2 at 4 h after Fe ions and a higher percentage were noticed 24 h later. Co-localization of Smad7 foci to RAD51, a protein important in HR repair (HRR) was observed in a small percentage of cells (Figure 2F), while all cells exposed to IR were noticed possessing Smad7 foci. These results suggest that Smad7 IRIF are formed in all phases of the cell cycle. The level of co-localization of Smad7 and Rad51 was relatively lower compared with that of pATF2 at both 4 and 24 h. To determine whether these findings were unique to this cell line, we performed similar studies in primary human fibroblasts (IMR90) (Figure 2E) and human hTERT-immortalized EPCs (Figure 6A) and found Smad7 foci localized with pATF2 at DSB sites. Since we were not able to detect residual IRIF 24 h after 1 Gy of γ -rays in EPC cells, 2 Gy of γ -rays was delivered to EPC cells to allow detection 24 h after exposure. Co-localization of Smad7 with proteins known to localize to the sites of DSB following irradiation likely indicates a role for Smad7 during the DSB repair process, and confirmation of these findings in different cell types including adult human fibroblasts, fetal human fibroblasts and human epithelial cells suggest the universality of the response.

ATM but not TGF β is dispensable for the formation of Smad7 foci

Upon DSB induction, the ATM kinase is known to be critical for IRIF formation. The effect of ATM kinase inhibition on Smad7 foci formation was investigated using a specific inhibitor of ATM, KU55933. Phosphorylation of ATF2, a known ATM substrate, was inhibited by

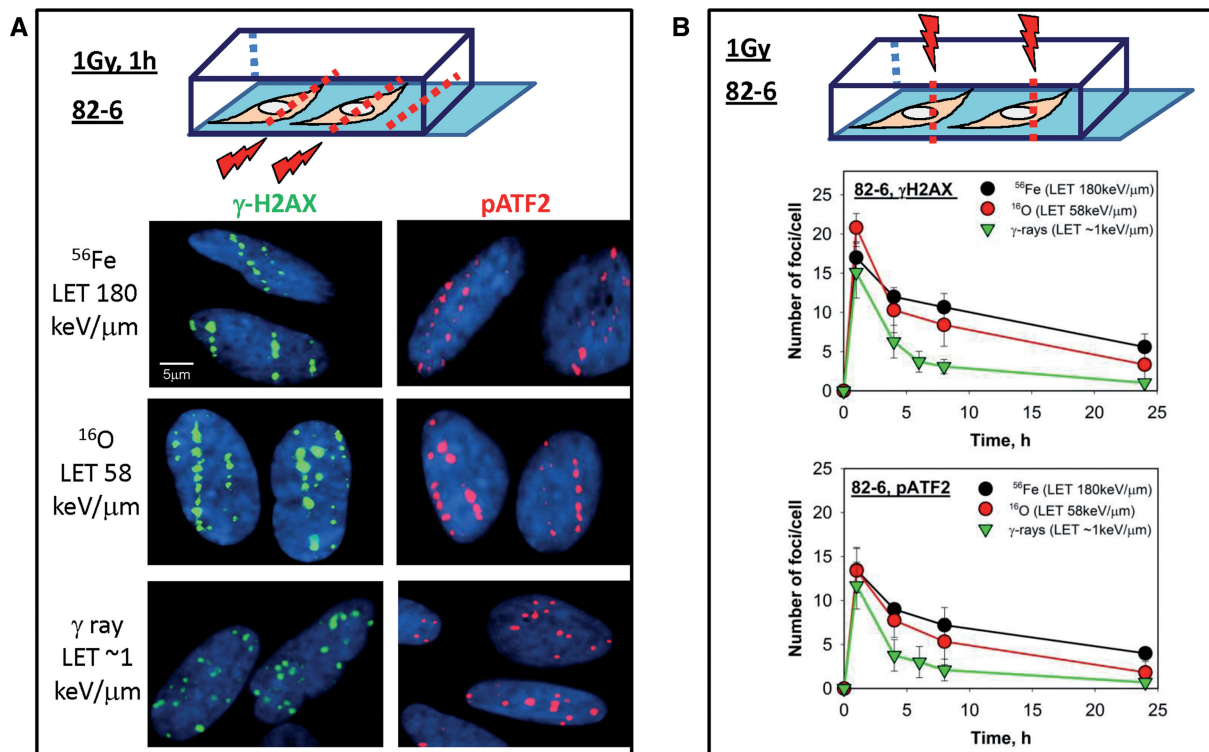


Figure 1. Kinetics of DSB repair protein foci formation after high versus low LET radiation in human fibroblasts. (A) Foci distribution based on radiation quality exposure. 82-6 cells cultured in chamber slides were irradiated horizontally to the beam axis at room temperature with Fe, O or γ -rays, of indicated LET values. One hour after a dose of 1 Gy, cells were fixed by paraformaldehyde and subsequently stained for immunofluorescence imaging. γ H2AX tracks of heavy ions passing through the cell nucleus are shown in green, and red foci tracks are obtained using pATF2-specific antibodies. DAPI staining (blue) represents cell nuclei. (B) Evaluation of γ H2AX and pATF2 foci decay in 82-6 cells as a function of time. As illustrated in the diagram in this set of experiments, cells were irradiated vertically to the beam axis so that individual foci rather than tracks would be visualized. At various times after irradiation, the number of foci in each cell nucleus was manually counted, results from two independent exposures were included and the average number of foci/cell was plotted. Non-irradiated cells were used as control. For each experiment, γ H2AX and pATF2 foci were counted in at least 100 cells.

KU55933 treatment following exposure to 1 Gy of γ -rays (Figure 3C); however, no significant difference in the formation of Smad7 foci between KU55933-treated cells and untreated cells was observed (Figure 3C). We confirmed independence of Smad7 focus formation on functional ATM by demonstrating Smad7 IRIF formation in ATM mutant cells (AT) following O particle exposure (Figure 3D), whereas pATF2 foci are absent in these cells following this exposure (Supplementary Figure S1).

Since Smad7 is known to interact with activated TGF β type I receptor to block TGF β /Smad activation (24), we attempted to confirm these findings in our cells using the TGF β type I receptor inhibitor-SD208 prior to radiation. The importance of TGF β signaling was clearly evident by the lack of radiation-induced Smad7 foci following SD208 treatment (Figure 3B). Neither KU55933 nor SD208 or dimethylsulfoxide (DMSO) (Figure 3A) treatment alone induced Smad7 foci in sham-irradiated cells.

Both Smad3 and Smad2 are upregulated after radiation, but only Smad 2 is observed at DSB sites

To investigate how the R-Smad members of the TGF β /Smad pathway, Smad2 and Smad3, respond to various radiation qualities, human fibroblasts were exposed to different types of radiation: Fe, O and γ -rays at a dose of

1 Gy and the presence of IRIF containing these proteins was studied. 53BP1 is another established DSB repair protein that can be seen to form prompt foci tracks 1 h after exposure to Fe (LET of 180 keV/ μ m), with \sim 6 foci per cell remaining 24 h after exposure in IMR90 cells (Figure 4A), pSmad2 did not form foci 1 h after radiation, in contrast to observation of Smad7 at this time, yet were observed at 4 h after exposure and were noted to co-localize with 53BP1, as well as γ H2AX, although the number of foci were less numerous than the 53BP1 and γ H2AX foci. The co-localization between pSmad2 and 53BP1 continued up until at least 24 h after exposure. Similar results were achieved in 82-6 (Figure 4B) and EPC cells (Figure 6B) following Fe ion exposure, as well as following exposure to O (LET of 58 keV/ μ m) and the low LET γ -rays. The decay kinetics of pSmad2 foci induced by exposure to different radiation qualities are shown in Figure 4D. pSmad2 foci showed similar kinetics as γ H2AX and pATF2, exhibiting a faster decay following γ -rays, and a slower decay following exposure to Fe and O particles, although the number of Smad2 foci formed are less than those of γ H2AX and pATF2. A cell cycle specificity for pSmad2 foci was noted by co-staining with cyclin A, a marker for S phase, which revealed pSmad2 foci were found mostly in non-S phase, mainly

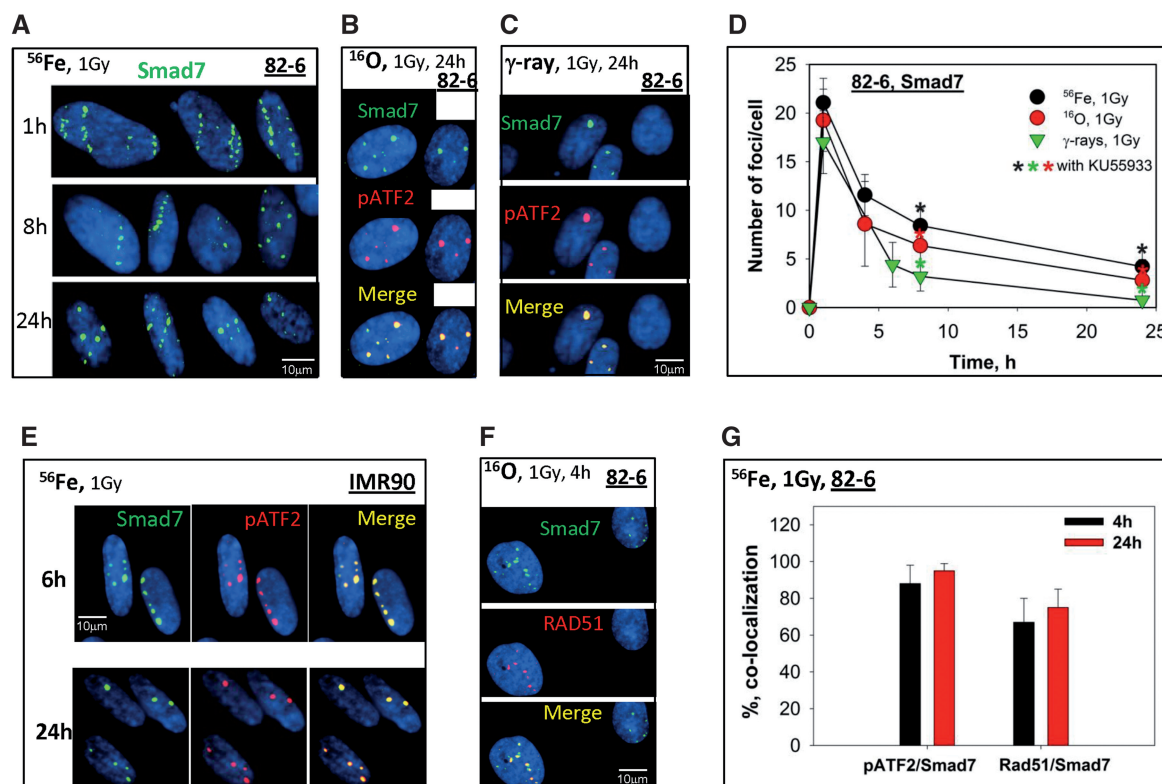


Figure 2. Smad7 focus formation triggered by IR in human fibroblasts and epithelial cells. (A) Smad7 foci (green) tracks in 82-6 cells fixed at 1, 8 and 24 h after 1 Gy of Fe ions exposure. Nuclei are visualized with DAPI staining. Cell slides were irradiated horizontally. (B) Co-localization of Smad7 (green) and pATF2 (red) 24 h after O ions exposure in 82-6 cells. (C) Co-localization of Smad7 (green) and pATF2 (red) 24 h after γ -rays in 82-6 cells. (D) Kinetics of Smad7 foci decay after Fe, O ions or γ -rays exposures in 82-6 cells. Asterisks indicate the results from KU55933 (ATM kinase inhibitor) inhibition, black: Fe; Red: O and green as for γ -rays. Cell slides were irradiated vertically. Two exposures were performed for each radiation type. Smad7 foci were counted in 100 cells for each experiment and averaged. (E) Co-localization of Smad7 (green) and pATF2 (red) in IMR90 cells after 1 Gy of Fe ions exposure at indicated times. (F) Co-localization of Smad7 (green) and RAD51 (red) 4 h after γ -rays in 82-6 cells. (G) Quantitative analysis of the level of co-localization of Smad7 with pATF2 or Rad51 4 or 24 h after Fe ions exposure.

G1 cells (Figures 4C and 6C). The levels of co-localization of pSmad2 with γ H2AX and 53BP1 were analyzed in Figure 3E, revealing that most of the DSBs repair proteins co-localized with pSmad2 (>80%) at 4 and 24 h after Fe ions exposure.

Results from western blot studies reveal that both p53 activation (Ser15) and Smad2 phosphorylation are increased in response to IR (Figure 4E and Supplementary Figure S2). As both Smad2 and Smad3 can form a complex with Smad4 following TGF β signaling, we examined the response of Smad3 to radiation. After high LET radiation, an increase in the total amount of Smad3 protein in the nucleus was found compared with non-irradiated 82-6 cells (Figure 4E and Supplementary Figure S2). However, pSmad3 did not form IRIF at DSBs following either high or low LET radiation exposure under our conditions employed.

ATM-dependent, but TGF β -independent Smad2 phosphorylation following IR

Activated TGF β has been shown to increase pSmad2 accumulation in the nucleus, resulting in a modification of the regulation of target gene expression. Since we observed IRIF-containing pSmad2, further experiments were performed to test for the TGF β dependence of these foci. A

rapid accumulation of pSmad2 was detected in nuclear extracts which could be abrogated by the TGF β R1 inhibition using SD208 (32), however no pSmad2 foci were observed after TGF β treatment alone, indicating a lack of dependence on TGF β without damage. The lack of TGF β dependence on IR-induced pSmad2 foci was confirmed using γ -rays (Figure 5A) and O particle irradiation (Figure 5B), suggesting Smad2 has a different mechanism of activation following radiation when compared with the classic TGF β /Smad activation pathway.

We then investigated the function of ATM in the induction of Smad2 phosphorylation after IR exposure. Upon ATM inhibitor (KU55933) treatment, no pSmad2 foci were observed 6–24 h following γ -rays, O and Fe particle exposures (Figure 5A). We confirmed these studies using AT cells and O particle exposure, and again observed pSmad2 foci to be absent throughout the repair period in AT cells, yet present in the wild-type cells at these same time points (Figure 5C and D).

DISCUSSION

The molecular basis for the cellular and tissue responses to IR including DNA repair, cell cycle regulation and tissue or organism responses is considered (1,4,18). The ATM

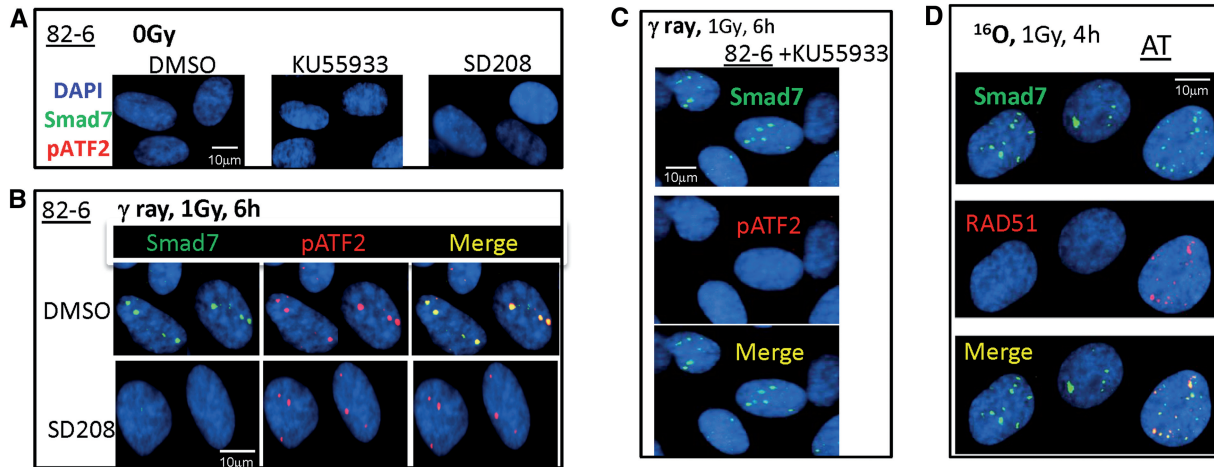


Figure 3. The effect of ATM kinase and TGF β receptor signaling on Smad7 foci formation after IR. (A) Sham-irradiated 82-6 cells were treated with KU55933, SD208 (TGF β R1 inhibitor) and DMSO (vehicle control) for 1 h before paraformaldehyde fixation. (B) 82-6 cells were pretreated with SD208 prior to 1 Gy of γ -rays. Shown are the foci co-localization of Smad7 (green) and pATF2 (red). (C) Same as (B), except cells were pretreated with KU55933. (D) Co-localization of Smad7 and RAD51 in AT cells after O ion exposure.

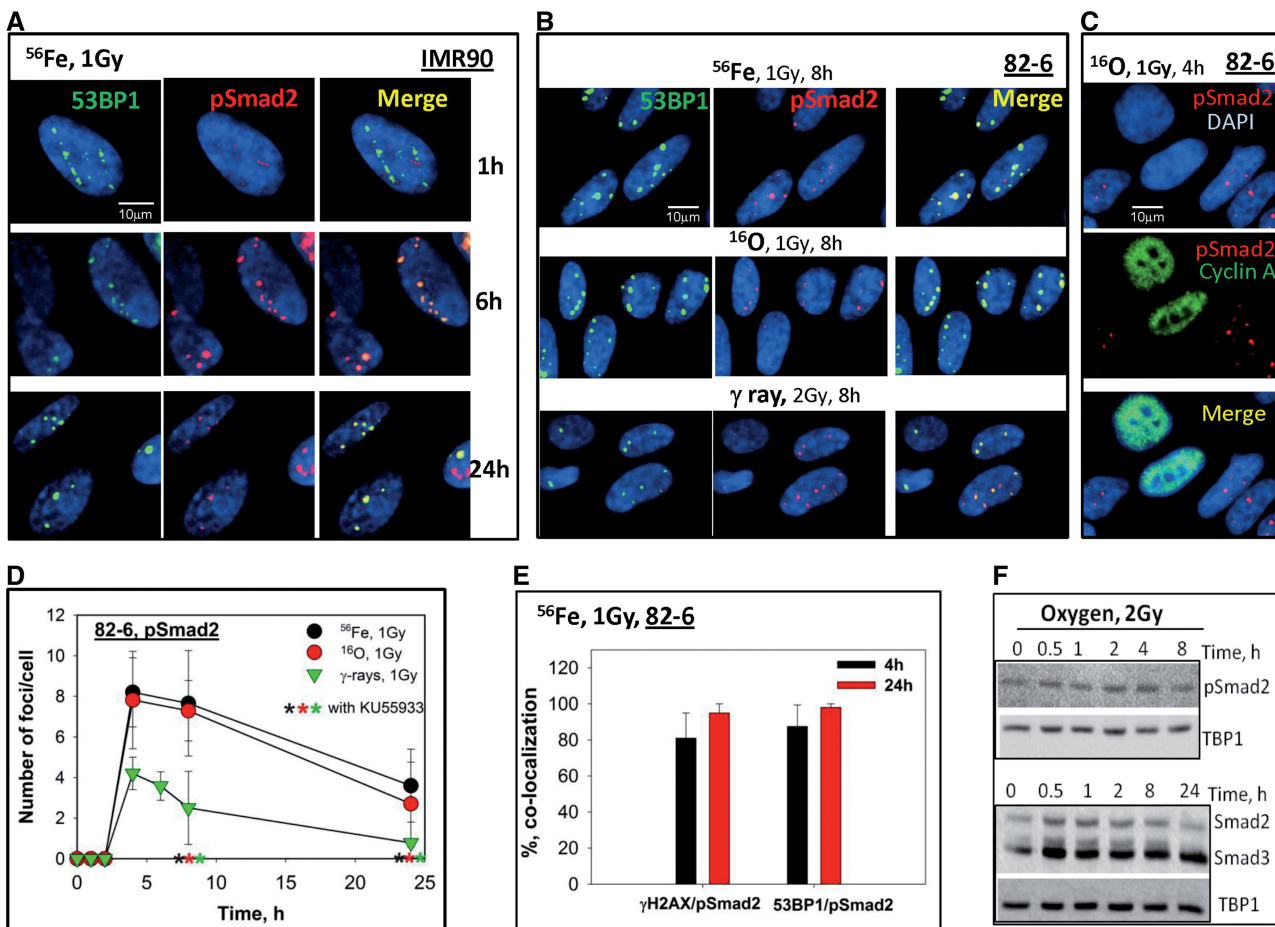


Figure 4. Phosphorylated Smad2 foci formation induced by IR in human fibroblast and epithelial cells. (A) Co-localization of 53BP1 (green) and pSmad2 (red) in IMR90 cells fixed at 1, 6 and 24 h after 1 Gy of Fe ions exposure. (B) Co-staining of 53BP1 (green) and pSmad2 (red) in 82-6 after 1 Gy of Fe, O ions or 2 Gy of γ -rays exposure. (C) Co-staining of pSmad2 (red) and cyclin A (green) in 82-6 cells 4 h after 1 Gy of O ions. (D) Kinetics of pSmad2 foci decay after irradiation with Fe, O ions or γ -rays in 82-6 cells as a function of time. Other details as in Figure 2E. (E) Quantitative analysis of the level of co-localization of pSmad2 with 53BP1 or γ H2AX 4 or 24 h after Fe ions exposure. (F) Nuclear extracts from 82-6 cells were prepared at different times after 2 Gy of O ions exposure. Phosphorylation of Smad2 as well as total Smad2/Smad3 were detected by western blotting. TBP1 was used as an internal control for nuclear extracts.

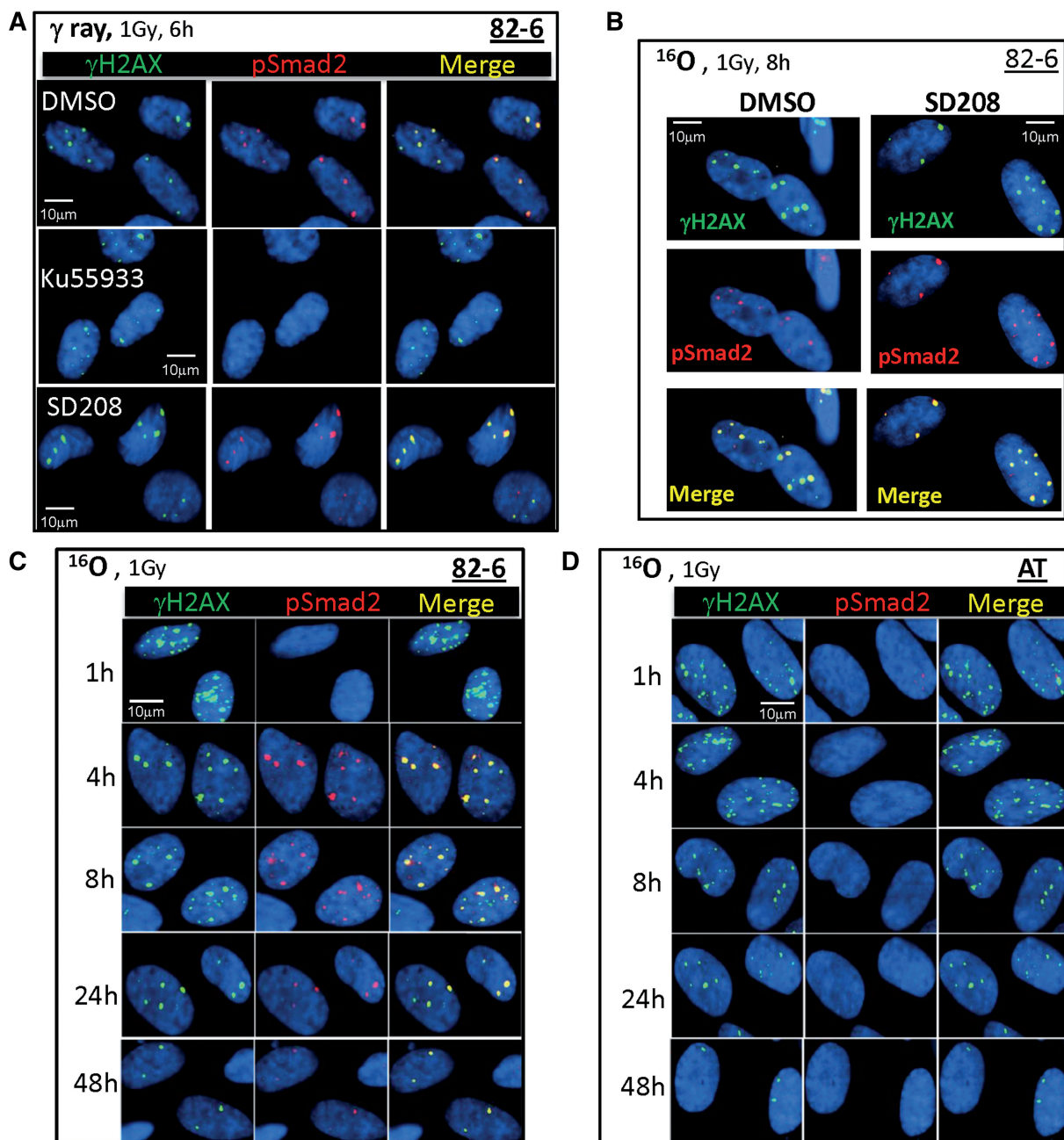


Figure 5. The effect of ATM kinase and TGF β receptor signaling on pSmad2 foci formation after IR. (A) 82-6 cells were pretreated with DMSO, SD208 or KU55933 for 1 h prior to 1 Gy of γ -rays. Shown are the foci co-localization of γ H2AX (green) and pSmad2 (red) 6 h after radiation. (B) 82-6 cells were pretreated with SD208 prior to 1 Gy of O ions. Other details as in (A). (C) Co-localization of γ H2AX (green) and pSmad2 (red) at various times after 1 Gy of O ions in normal fibroblasts (82-6) and in (D) AT cells. Slides were irradiated vertical to the beam axis for these experiments.

pathway is known to play major roles in DDR to radiation, thus individuals with defects in ATM are extremely radiosensitive (33,34). TGF β signaling also appears to be important for cellular response to radiation (35), including tissue injury, growth inhibition, fibrosis and apoptosis (32,36–41). The current work has focused on understanding possible interactions between the ATM and TGF β signaling pathways following different radiation quality exposures in order to vary the contribution of complex DSBs. Smad proteins are key TGF β type I

receptor substrates which can transduce extracellular signals from TGF β to the nucleus and aid in the transcriptional regulation of certain genes.

Smad proteins have also been studied by several groups (27,42) and demonstrated to increase in expression following IR. However, little work to date has been done looking at the relationship between Smad protein kinetics and the kinetics for various DNA DSB repair proteins at DSB sites. Following localized small intestinal irradiation, a progressively increased Smad3 mRNA level

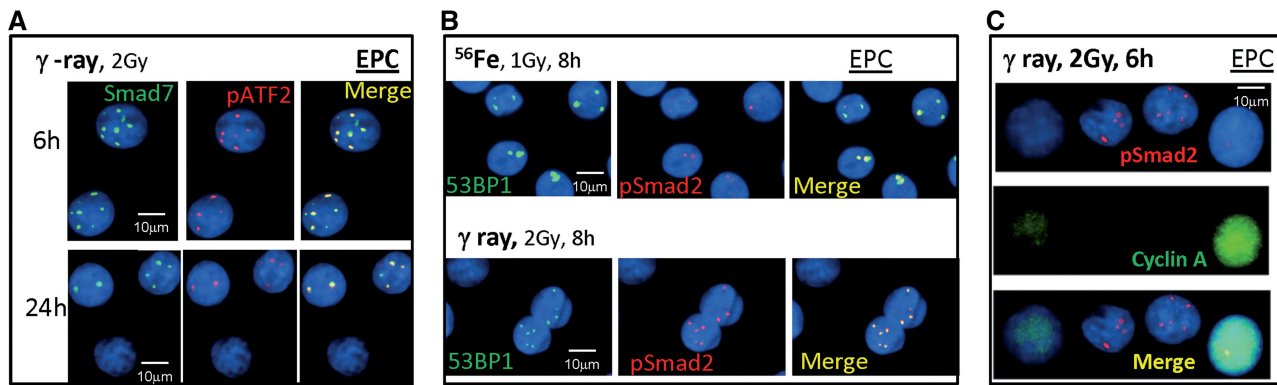


Figure 6. Smad7 and pSmad2 focus formation triggered by IR in human epithelial cells. (A) Smad7 foci (green) co-localize with pATF2 in EPC cells fixed at 6 and 24 h after 2 Gy of γ -rays. (B) Co-localization of pSmad2 and 53BP1 foci after 1 Gy of Fe ions and 2 Gy of γ -rays. (C) Co-staining of pSmad2 (red) and cyclin A (green) in EPC cells 6 h after 2 Gy of γ -rays.

was observed but not inhibitory Smad7 (43). Others have observed persistent increasing of Smad7 expression as a result of IR exposure (44,45). Phosphorylation of Smad2 and Smad3 and translocation from cytoplasm to nucleus in the response to IR have been detected in several studies involving rat tissue as well as cell lines (27,46–48). Down-regulation of Smad 1/5/8 activation was observed after 10 Gy of IR (46). Moreover, tumor suppressor p53 is known as a direct sensor to IR, and the fact that Smad2/3 and p53 physically interact implies that p53 activation might serve as a bridge connecting TGF β signaling and IR responses (49). The studies above demonstrated the response of Smad proteins to IR through the activation of TGF β , while the direct effect of Smad proteins to DNA damage induced by IR such as DNA repair was not revealed.

Uniquely, we observe co-localization of phosphorylated Smad2 (S465/S467) and Smad7, but not Smad3, with DSB repair proteins (e.g. γ H2AX, 53BP1, pATF2 and RAD51) in both human epithelial and fibroblast cells following both γ -ray and high LET particle irradiation at moderate doses. High LET particles resulted in foci tracks containing both pSmad2 and Smad7, and the disappearance of these foci was delayed when compared with γ -rays. Smad7 foci formed promptly after radiation (detected as early as 1 h after IR), while pSmad2 foci were not detectable until 4 h after exposure. The time course of resolution of pSmad2 and Smad7 foci was similar to that of γ H2AX and 53BP1 foci. Co-localization of Smad7 with the HRR protein-RAD51 was observed in G2 cells, although Smad7 foci were detected in other phases of the cell cycle as well. In contrast, pSmad2 foci were observed primarily in G1 cells. The observation that pSmad2 is mainly observed in G1 cells might be explained by pSmad2 primarily participating in the NHEJ pathway or playing a role in the G1/S checkpoint in addition to its transcription factor role. The late appearance of pSmad2 needs to be further investigated. The relatively early appearance of Smad7 foci perhaps indicates a possible direct binding to DSB breaks, whereas pSmad2, which is unable to directly bind DNA, is likely to be indirectly localized to DSB sites through interactions with other repair molecules at a later

stage, perhaps as a result of chromatin remodeling during repair or an additional role in transcription activation.

ATM signaling is essential for optimal cellular and tissue response to IR. To further characterize the potential role for pSmad2 in DDR, we investigated how ATM kinase activity is related to pSmad2 kinetics. It is well established that ATF2 (Ser490/498) is a phosphorylation target of ATM involved in DDR following IR (12,13). To confirm the ATM dependence of pATF2 foci, we used both an ATM kinase inhibitor and AT cells and monitored the formation of radiation-induced pATF2 foci. pATF2 foci were not observed in cells treated with ATM kinase inhibitor nor in the AT cells supporting the ATM dependence of ATF2 activation at the Ser490/498 site. We then used the same strategy to investigate the dependence of pSmad2 foci on ATM kinase activity. Similar to pATF2, complete abrogation of pSmad2 focus formation was observed both by addition of the ATM kinase inhibitor as well as in the ATM mutant cells. Thus, this work reveals for the first time that Smad2 is a phosphorylation target of ATM in response to IR-induced DNA damage.

We further tested the TGF β dependence of pSmad2 foci using a TGF β R1 inhibitor and noted that pSmad2 foci formation was not diminished with this treatment. Together these data indicate that a fraction of Smad2 phosphorylation is ATM dependent. Furthermore, since pSmad2 and pSmad3 can form heteromeric complexes upon TGF β stimulation (19,22), we also investigated how kinetics of pSmad3 foci compared with pSmad2 following IR. However, unlike pSmad2, which showed a delay in co-localization with DSB proteins, neither total Smad3 nor pSmad3 was observed to form foci and co-localize with other DSB proteins at DSBs. Smad3 co-localization to DSB proteins had been observed previously using DNA damage reagents or at very high doses (>10 Gy) (50). Additionally, unpublished data from our group and others (27) have noted that activation of ATM following IR is independent of TGF β R1 signaling, and these results would support pSmad2 also having a TGF β signaling-independent role following radiation-induced damage. Smad7 foci formed promptly after radiation,

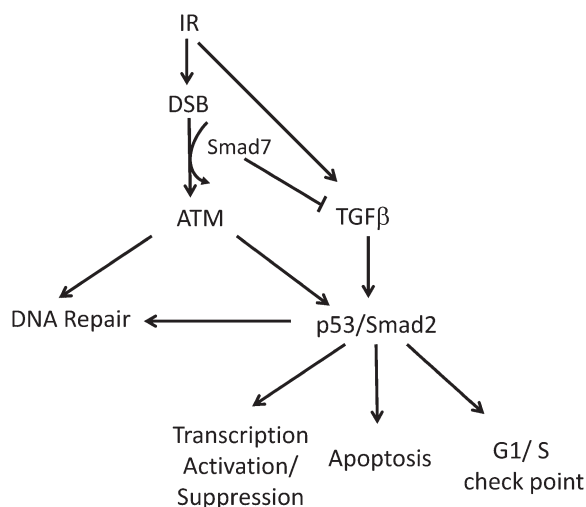


Figure 7. Proposed model for the role of Smad2 and Smad7 in response to IR-induced DSBs and relationship to ATM and TGF β pathways.

however, were not inhibited upon ATM inhibitor treatment or diminished in AT cells. However, when cells were pretreated with TGF β R1 inhibitor, Smad7 foci were not visible after radiation, indicating a TGF β dependence unlike pSmad2 foci.

A schematic model based on our new findings combined with previous understanding of the roles of Smad2 and Smad7 in the DDR, and the crosstalk that occurs between the TGF β /Smad and ATM response pathways is presented in Figure 7. It has been shown that p53 physically interacts with Smad2 (49,51). Phosphorylated Smad2 is a target of ubiquitin Smurf2 after translocation into nucleus, and based on other's studies, Smurf2 foci can be observed to co-localize with DSB proteins and stay elevated up to months after high LET radiation (52). Smad2 could act as a potential tumor suppressor (53), with loss of the protein resulting in an increase in the risk of cell malignancy. Understanding the mechanisms for Smad2 foci formation for different radiation qualities and doses after IR will aid in understanding the role of Smad2 in radiation effects.

Overall, our study reveals for the first time that two Smad proteins, Smad7 and pSmad2, localize to IR-induced DSBs, albeit with differential kinetics (Figure 7). We identified that IR-induced phosphorylation of Smad2 is ATM-dependent; whereas Smad7 focus formation is TGF β 1 receptor dependent following radiation exposure. Smad2 and Smad7, as a potential tumor suppressor and oncogene, respectively, are involved in the DNA damage signaling pathway. Finally, our studies revealing a delayed disappearance of pSmad2 and Smad7 foci after high LET particle exposure may also indicate an increased biological effectiveness and carcinogenic risk for high LET radiation (54).

SUPPLEMENTARY DATA

Supplementary Data are available at NAR Online: Supplementary Figures 1 and 2.

ACKNOWLEDGEMENTS

The authors thank for the team of Medical and Accelerator Departments at BNL for support at NSRL and Ms Christine Cucinotta for help with editing the article.

FUNDING

The NASA Space Radiation Program and US Department of Energy [DE-AI02-10ER64969 and DE-SC0002296]. Funding for open access charge: NASA.

Conflict of interest statement. None declared.

REFERENCES

- Jackson,S.P. and Bartek,J. (2009) The DNA-damage response in human biology and disease. *Nature*, **461**, 1071–1078.
- Goodhead,D.T., Thacker,J. and Cox,R. (1993) Effects of radiations of different qualities on cells: molecular mechanisms of damage and repair. *Int. J. Radiat. Biol.*, **63**, 543–556.
- Cucinotta,F.A., Nikjoo,H. and Goodhead,D.T. (2000) Model of the radial distribution of energy imparted in nanometer volumes from HZE particle. *Radiat. Res.*, **153**, 459–468.
- Prise,K.M., Pinto,M., Newman,H.C. and Michael,B.D. (2001) A review of studies of ionizing radiation-induced double-strand break clustering. *Radiat. Res.*, **156**, 572–576.
- Feinendegen,L.E. (2002) Reactive oxygen species in cell responses to toxic agents. *Hum. Exp. Toxicol.*, **21**, 85–90.
- Ma,Y., Lu,H., Tippin,B., Goodman,M.F., Shimazaki,N., Koiwai,O., Hsieh,C.L., Schwarz,K. and Lieber,M.R. (2004) A biochemically defined system for mammalian nonhomologous DNA end joining. *Mol. Cell*, **16**, 701–713.
- Wang,H., Zeng,Z.C., Perrault,A.R., Cheng,X., Qin,W. and Iliakis,G. (2001) Genetic evidence for the involvement of DNA ligase IV in the DNA-PK-dependent pathway of non-homologous end joining in mammalian cells. *Nucleic Acids Res.*, **29**, 1653–1660.
- Anderson,J.A., Harper,J.V., Cucinotta,F.A. and O'Neill,P. (2010) Participation of DNA-PKs in DSB repair following exposure to high- and low-LET radiation. *Radiat. Res.*, **174**, 195–205.
- Wang,M., Wu,W., Wu,W., Rosidi,B., Zhang,L., Wang,H. and Iliakis,G. (2006) PARP-1 and Ku compete for repair of DNA double strand breaks by distinct NHEJ pathways. *Nucleic Acids Res.*, **34**, 6170–6182.
- Baumann,P. and West,S.C. (1998) Role of the human RAD51 protein in homologous recombination and double-stranded-break repair. *Trends Biochem. Sci.*, **23**, 247–251.
- Riballo,E., Kuhne,M., Rief,N., Doherty,A., Smith,G.C., Recio,M.J., Reis,C., Dahm,K., Fricke,A., Krempler,A. et al. (2004) A pathway of double-strand break rejoining dependent upon ATM, Artemis and proteins locating to γ -H2AX foci. *Mol. Cell*, **16**, 715–724.
- Fernandez-Capetillo,O., Celeste,A. and Nussenzweig,A. (2003) Focusing on foci: H2AX and the recruitment of DNA-damage response factors. *Cell Cycle*, **2**, 426–427.
- Rappold,I., Iwabuchi,K., Date,T. and Chen,J. (2001) Tumor suppressor p53 binding protein 1 (53BP1) is involved in DNA damage-signaling pathways. *J. Cell Biol.*, **153**, 613–620.
- Bhoumik,A., Takahashi,S., Breitweiser,W., Shiloh,Y., Jones,N. and Ronai,Z. (2005) ATM-dependent phosphorylation of ATF2 is required for the DNA damage response. *Mol. Cell*, **18**, 577–587.
- Whalen,M.K., Gurai,S.K., Zahed-Kargar,H. and Pluth,J.M. (2008) Specific ATM-mediated phosphorylation dependent on radiation quality. *Radiat. Res.*, **150**, 353–364.
- Cucinotta,F.A., Pluth,J.M., Anderson,J.A., Harper,J.V. and O'Neill,P. (2008) Biochemical Kinetics model of DSB repair and induction of γ -H2AX foci by non-homologous end joining. *Radiat. Res.*, **169**, 214–222.

17. Kinner, A., Wu, W., Staudt, C. and Iliakis, G. (2008) γ -H2AX in recognition and signaling of DNA double-strand breaks in the context of chromatin. *Nucleic Acids Res.*, **36**, 5678–5694.
18. Kirshner, J., Jobling, M.F., Pajares, M.J., Ravani, S.A., Glick, A.B., Lavin, M.J., Koslov, S., Shiloh, Y. and Barcellos-Hoff, M.H. (2006) Inhibition of transforming growth factor-beta1 signaling attenuates ataxia telangiectasia mutated activity in response to genotoxic stress. *Cancer Res.*, **66**, 10861–10869.
19. Derynck, R., Akhurst, R.J. and Balmain, A. (2001) TGF β signaling in tumor suppression and cancer progression. *Nat. Genet.*, **29**, 117–129.
20. Derynck, R. and Zhang, Y.E. (2003) Smad-dependent and Smad-independent pathways in TGF-beta family signalling. *Nature*, **425**, 577–584.
21. Levy, L. and Hill, C.S. (2005) Smad4 dependency defines two classes of transforming growth factor beta target genes and distinguishes TGF β -induced epithelial-mesenchymal transition from its antiproliferative and migratory responses. *Mol. Cell Biol.*, **25**, 8108–8125.
22. Inman, G.J., Nicolas, F.J. and Hill, C.S. (2002) Nucleocytoplasmic shuttling of Smads 2, 3, and 4 permits sensing of TGF-beta receptor activity. *Mol. Cell*, **10**, 283–294.
23. Mavrakis, K.J., Andrew, R.L., Lee, K.L., Petropoulou, C., Dixon, J.E., Navaratnam, N., Norris, D.P. and Episkopou, V. (2007) Arkadia enhances Nodal/TGF- β signaling by coupling phospho-Smad2/3 activity and turnover. *PLoS Biol.*, **5**, e67.
24. Nakao, A.M., Nakao, A., Afrakhte, M., Morén, A., Nakayama, T., Christian, J.L., Heuchel, R., Itoh, S., Kawabata, M., Heldin, N.E. *et al.* (1997) Identification of Smad7 a TGFbeta-inducible antagonist of TGF-beta signaling. *Nature*, **389**, 631–635.
25. Hayashi, H., Abdollah, S., Qiu, Y., Cai, J., Xu, Y.Y., Grinnell, B.W., Richardson, M.A., Topper, J.N., Gimbrone, M.A.J., Wrana, J.L. *et al.* (1997) The MAD-related protein Smad7 associates with the TGFbeta receptor and functions as an antagonist of TGFbeta signaling. *Cell*, **9**, 1165–1173.
26. Zhang, S., Ekman, M., Thakur, N., Bu, S., Davoodpour, P., Grimsby, S., Tagami, S., Heldin, C.H. and Landström, M. (2006) TGFbeta1-induced activation of ATM and p53 mediates apoptosis in a Smad7-dependent manner. *Cell Cycle*, **5**, 2787–2795.
27. Wiegman, E.M., Blaese, M.A., Loeffler, H., Coppes, R.P. and Rodemann, H.P. (2007) TGFbeta1 dependent fast stimulation of ATM and p53 phosphorylation following exposure to ionizing radiation does not involve TGFbeta-receptor I signaling. *Radiother. Oncol.*, **83**, 289–295.
28. Yannone, S.M., Roy, S., Chan, D.W., Murphy, M.B., Huang, S., Campisi, J. and Chen, D.J. (2001) Werner syndrome protein is regulated and phosphorylated by DNA-dependent protein kinase. *J. Biol. Chem.*, **276**, 38242–38248.
29. Wang, M., Hada, M., Huff, J., Pluth, J., Anderson, J., O'Neill, P. and Cucinotta, F.A. (2012) Heavy ions can enhance TGF β mediated epithelial to mesenchymal transition. *J. Radiat. Res.*, **53**, 51–57.
30. Desai, N., Davis, E., O'Neill, P., Durante, M., Cucinotta, F.A. and Wu, H. (2005) Immunofluorescent detection of DNA double strand breaks induced by high-LET radiation. *Radiat. Res.*, **164**, 518–521.
31. Ponomarev, A., Huff, J. and Cucinotta, F.A. (2010) The analysis of the densely populated patterns of radiation-induced foci by a stochastic, Monte Carlo model of DNA double strand breaks induction by heavy ions. *Int. J. Radiat. Biol.*, **86**, 507–515.
32. Wang, M., Hada, M., Saha, J., Sridharan, D.M., Pluth, J. and Cucinotta, F.A. (2012) Protons sensitize epithelial to mesenchymal transition. *PLoS One*, **7**, e41249.
33. Gilad, S., Khosravi, R., Shkedy, D., Uziel, T., Ziv, Y., Savitsky, K., Rotman, G., Smith, S., Chessa, L., Jorgensen, T.J. *et al.* (1996) Predominance of null mutations in ataxia-telangiectasia. *Hum. Mol. Genet.*, **5**, 433–439.
34. Hada, M., Huff, J.L., Patel, Z.S., Kawata, T., Pluth, J.M., George, K.A. and Cucinotta, F.A. (2011) AT cells are not radiosensitive for simple chromosomal exchanges at low dose. *Mutat. Res.*, **716**, 76–83.
35. Barcellos-Hoff, M.H. (1998) How do tissues respond to damage at the cellular level? The role of cytokines in irradiated tissues. *Radiat. Res.*, **150**, S109–S120.
36. Tian, M., Neil, J.R. and Schiemann, W.P. (2011) Transforming growth factor- β and the hallmarks of cancer. *Cell. Signal.*, **23**, 951–962.
37. Li, M.O., Wan, Y.Y., Sanjabi, S., Robertson, A.K. and Flavell, R.A. (2006) Transforming growth factor-beta regulation of immune responses. *Annu. Rev. Immunol.*, **24**, 99–146.
38. Ehrhart, E.J., Segarini, P., Tsang, M.L., Carroll, A.G. and Barcellos-Hoff, M.H. (1997) Latent transforming growth factor beta1 activation in situ: quantitative and functional evidence after low-dose gamma-irradiation. *FASEB J.*, **11**, 991–1002.
39. Barcellos-Hoff, M.H., Derynck, R., Tsang, M.L. and Weatherbee, J.A. (1994) Transforming growth factor-beta activation in irradiated murine mammary gland. *J. Clin. Invest.*, **93**, 892–899.
40. Kruse, J.J., Floom, B.G., te Poele, J.A., Russell, N.S. and Stewart, F.A. (2009) Radiation-induced activation of TGF-beta signaling pathways in relation to vascular damage in mouse kidneys. *Radiat. Res.*, **171**, 188–197.
41. Ewan, K.B., Henshall-Powell, R.L., Ravani, S.A., Pajares, M.J., Arteaga, C., Warters, R., Akhurst, R.J. and Barcellos-Hoff, M.H. (2002) Transforming growth factor-beta1 mediates cellular response to DNA damage in situ. *Cancer Res.*, **62**, 5627–5631.
42. Yano, H., Hamanaka, R., Nakamura, M., Sumiyoshi, H., Matsuo, N. and Yoshioka, H. (2012) Smad, but not MAPK, pathway mediates the expression of type I collagen in radiation induced fibrosis. *Biochem. Biophys. Res. Commun.*, **418**, 457–463.
43. Hneino, M., François, A., Buard, V., Tarlet, G., Abderrahmani, R., Bliorando, K., Hoodless, P.A., Benderitter, M. and Milliat, F. (2012) The TGF- β /Smad repressor TG-interacting factor 1 (TGIF1) plays a role in radiation-induced intestinal injury independently of a smad signaling pathway. *PLoS One*, **7**, e35672.
44. Kruse, J.J., Floom, B.G., te Poele, J.A., Russell, N.S. and Stewart, F.A. (2009) Radiation-induced activation of TGF- β signaling pathways in relation to vascular damage in mouse kidneys. *Radiat. Res.*, **171**, 188–197.
45. Dancea, H.C., Shareef, M.M. and Ahmed, M.M. (2009) Role of radiation-induced TGF-beta signaling in cancer therapy. *Mol. Cell Pharmacol.*, **1**, 44–56.
46. Scharpfenecker, M., Kruse, J.J., Sprong, D., Russell, N.S., Ten Dijke, P. and Stewart, F.A. (2009) Ionizing radiation shifts the PAI-1/ID-1 balance and activates notch signaling in endothelial cells. *Int. J. Radiat. Oncol. Biol. Phys.*, **73**, 506–513.
47. Chen, L., Brizel, D.M., Rabbani, Z.N., Samulski, T.V., Farrell, C.L., Larrier, N., Anscher, M.S. and Vujaskovic, Z. (2004) The protective effect of recombinant human keratinocyte growth factor on radiation-induced pulmonary toxicity in rats. *Int. J. Radiat. Oncol. Biol. Phys.*, **60**, 1520–1529.
48. Imaizumi, N., Monnier, Y., Hegi, M., Mirimanoff, R.O. and Rüegg, C. (2010) Radiotherapy suppresses angiogenesis in mice through TGF-betaRI/ALK5-dependent inhibition of endothelial cell sprouting. *PLoS One*, **5**, e11084.
49. Cordenonsi, M., Dupont, S., Maretto, S., Insinga, A., Imbriano, C. and Piccolo, S. (2003) Links between tumor suppressors: p53 is required for TGF-beta gene responses by cooperating with Smads. *Cell*, **113**, 301–314.
50. Dubrovskaya, A., Kanamoto, T., Lomnytska, M., Heldin, C.H., Volodko, N. and Souchelnytskyi, S. (2005) TGFbeta1/Smad3 counteracts BRCA1-dependent repair of DNA damage. *Oncogene*, **24**, 2289–2297.
51. Elston, R. and Inman, G.J. (2012) Crosstalk between p53 and TGF- β signaling. *J. Signal Transduct.*, **2012**, 294097.
52. Blank, M., Tang, Y., Yamashita, M., Burkett, S.S., Cheng, S.Y. and Zhang, Y.E. (2012) A tumor suppressor function of Smurf2 associated with controlling chromatin landscape and genome stability through RNF20. *Nat. Med.*, **18**, 227–234.
53. Prunier, C., Mazars, A., Noe, V., Bruyneel, E., Mareel, M., Gespach, C. and Atfi, A. (1999) Evidence that Smad2 is a tumor suppressor implicated in the control of cellular invasion. *J. Biol. Chem.*, **274**, 22919–22922.
54. Cucinotta, F.A. and Durante, M. (2006) Cancer risk from exposure to galactic cosmic rays: implications for space exploration by human beings. *Lancet Oncol.*, **7**, 431–435.